ELSEVIER

Surface Science 343 (1995) 211–220

surface science

Electronic factors determining the reactivity of metal surfaces

B. Hammer [a,b,*], J.K. Nørskov [a]

[a] *Center for Atomic-Scale Materials Physics and Physics Department, Technical University of Denmark, DK-2800 Lyngby, Denmark*
[b] *Joint Research Center for Atom Technology, 1-1-4 Higashi, Tsukuba, Ibaraki 305, Japan*

Received 8 June 1995; accepted for publication 21 August 1995

Abstract

Based on density functional theory calculations of H_2 dissociation on Al(111), Cu(111), Pt(111) and $Cu_3Pt(111)$ we present a consistent picture of some key physical properties determining the reactivity of metal and alloy surfaces. The four metal surfaces are chosen to represent metals with no *d*-bands, with filled *d*-bands and with *d*-states at the Fermi level. We show that electronic states in the entire valence band of the metal surface are responsible for the reactivity, which consequently cannot be understood solely in terms of the density of states at the Fermi level nor in terms of the empty *d*-states above it. Rather we suggest that trends in reactivities can be understood in terms of the hybridization energy between the bonding and anti-bonding adsorbate states and the metal *d*-bands (when present), and we demonstrate that a simple frozen potential based estimate of the hybridization energy correlates well with the calculated variation of the barrier height for the different metal surfaces.

Keywords: Alloys; Chemisorption; Copper; Density functional calculations; Hydrogen; Models of surface chemical reactions; Platinum; Surface chemical reaction

1. Introduction

It is one of the long term goals of surface science to establish an understanding of the important physical properties of a surface determining its chemical reactivity. Such an understanding could be the basis for an "atomistic engineering" of surfaces with desired catalytic activity or selectivity. Two simple properties of the surface which have been successfully correlated with its reactivity are the local density of one-electron states at the Fermi level LDOS(E_F) [1–3] and the number of holes N_h in the *d*-bands [4]. More general formulations of surface reactivity measures based on concepts from the theory of gas phase chemical reactivity [5,6] have recently been developed [7], which give the two simple measures, LDOS(E_F) and N_h, as limiting cases of a more general dependence of the reactivity on the surface local density of states [8].

In the present paper, we present calculations of the energy along the reaction path for a set of systems selected to test out these concepts. The calculations are based on the density functional theory (DFT) total energy method. We choose the dissociation of H_2 as a test reaction and consider four metal surfaces Al(111), Cu(111), Pt(111) and $Cu_3Pt(111)$ chosen to illustrate metal surfaces with and without *d*-bands, with large and small Fermi level surface density of states LDOS(E_F) and with and without *d*-holes. We conclude that neither of the two simple reactivity measures are sufficient to understand all the systems. The $Cu_3Pt(111)$ surface

* Corresponding author. Fax: +45 45 93 23 99; E-mail: hammer@fysik.dtu.dk.

SSDI 0039-6028(95)00000-0

which we find to have essentially no d-holes just above the Fermi level and a low LDOS(E_F) is found to be as reactive as the Pt(111) surface, where there are both d-holes and a large LDOS(E_F). Instead we discuss our results in terms of the d-hybridization picture originally proposed in Refs. [9] and [10] and recently explicitly demonstrated to be of relevance in studies of H_2 dissociation on NiAl(110) and on the late transition and noble metal surfaces [11,12]. We show that the d-hybridization picture which associates the trends in reactivity with the *extra* hybridization between the metal d-states and adsorbate states that are renormalized due to the interaction with the metal sp states can be used to understand all the effects observed. We establish this by studying in detail the differences of the densities of states of the molecule outside the surfaces. We show that to understand the trends in the reactivities of all the surfaces it is important to include the interaction between the metal d-states and both the bonding and the anti-bonding molecular states. In particular, we show that whether or not a barrier for the dissociation exists is determined by the relative position in energy of the renormalized adsorbate states and metal d-bands, the molecule–surface s–d coupling matrix element, and the degree of filling of the molecule–surface anti-bonding states. Based on the effective medium theory [13] we formulate an approximate quantitative measure of the role of the d-hybridization on the barrier height and we demonstrate how this measure correlates with the barrier heights found in the full, self-consistent calculations.

2. Method

Density functional theory with the local density approximation (LDA) augmented by non-local terms (GGA) for the description of exchange-correlation effects [14,15] has been shown recently to describe adsorption and dissociation of simple molecules on metal surfaces semi-quantitatively [16–19]. For H_2 dissociation over Cu(111), for instance, the experimentally determined barrier is reproduced to within 0.1 eV [16,20]. In the present paper, we use the DFT to describe H_2 dissociation on a number of metal surfaces, which we choose to describe in a (repeated) slab geometry. An obvious advantage of this choice is that the metal states are inherently extended Bloch states. The main drawback of the slab geometry is that a complete array of molecules rather than just one single H_2 is reacting with the surface. The error introduced by this can, however, be controlled by systematically increasing the surface cell size.

The elemental metals Al, Cu, and Pt have fcc structure, while Cu_3Pt has the fcc-like Cu_3Au structure. The $Cu_3Pt(111)$ surface is known experimentally to show a (2×2) LEED pattern indicative of the surface being bulk stoichiometric with 25% Pt and 75% Cu in the first surface layer [21]. In the present theoretical work, the surfaces are all realized with super cells having a (2×2) surface unit cell, comprising six (111) layers of substrate atoms and five "empty" layers (i.e. >10 Å) of vacuum. Considering the small relaxations observed for the close-packed (111) fcc metal surfaces [22] we choose to use the truncated bulk positions neglecting the relaxations. H_2 is adsorbed on one slab surface and the difference in workfunctions of the two slab surfaces is compensated for by a dipole layer in the middle of the vacuum [23]. Using the methods of Payne, Teter and co-workers [24] and of Gillan [25], the Kohn–Sham equations are solved in a basis of plane waves of kinetic energy up to 50 Ry at 6 or 15 Bloch wave vectors (k-points) in the C_{3v} and C_{2v} irreducible Brillouin zones respectively. The vectors are chosen according to the method of Chadi and Cohen [26] and correspond to a total of 54 vectors in the $k_z=0$ plane of the entire first Brillouin zone. Fermi distributed occupation numbers at $kT_e=0.1$ eV are used to stabilize the iterative procedures and all total energies are extrapolated to 0 K [25]. The proton is described with the Coulomb potential, Al with a Bachelet–Hamann–Schlüter [27] pseudopotential, while for Cu and Pt the soft, scalar-relativistic pseudopotentials of Troullier and Martins [28] are used. The charge density and the density of states are found self-consistently within the LDA, as are the theoretical lattice constants, $a_{Al}=3.96$ Å, $a_{Cu}=3.57$ Å, $a_{Pt}=3.93$ Å, and $a_{Cu_3Pt}=$

3.68 Å used throughout this work. All total energies reported are GGA values derived from the LDA densities.

3. Reaction energetics

Fig. 1A summarizes the calculated energetics of H_2 outside the (111) surfaces of Al, Cu, Pt, and Cu_3Pt. In order to facilitate the qualitative and quantitative discussion of the trends in the H_2 dissociation over the different metal surfaces, we choose to study the H_2 in the same reaction geometry and for one fixed set of (b, Z) coordinates over all the surfaces. The atop dissociation with the two hydrogen atoms going into the third nearest neighbor three-fold sites is chosen as this simplifies the discussion of the molecule–surface interaction, by mainly involving one surface atom (cf. Figs. 1B–1D).

A large barrier is seen to build up towards dissociation over the Al(111) and Cu(111) surfaces [16] and over the Cu sites in Cu_3Pt(111). The Pt(111) and the Pt sites in Cu_3Pt(111), on the other hand, dissociate the H_2 without a barrier. For the Cu(111) surface where the adsorption is activated, we have checked the influence of the chosen reaction path by also allowing the molecule to find the minimum energy path [16]. This is shown by the dotted line in Fig. 1A. While the barrier is lower than for the fixed path, the inclusion of relaxations does not alter the trends seen for the unrelaxed calculations [29]. For the non-activated cases even lower energy paths might exist, but this would again not change the trends. We note that all features of the calculated potentials are in agreement with experiment. Cu and Al surfaces show a large barrier for dissociation [30,31] while H_2 dissociation occurs spontaneously on Pt and Cu_3Pt surfaces [21,32].

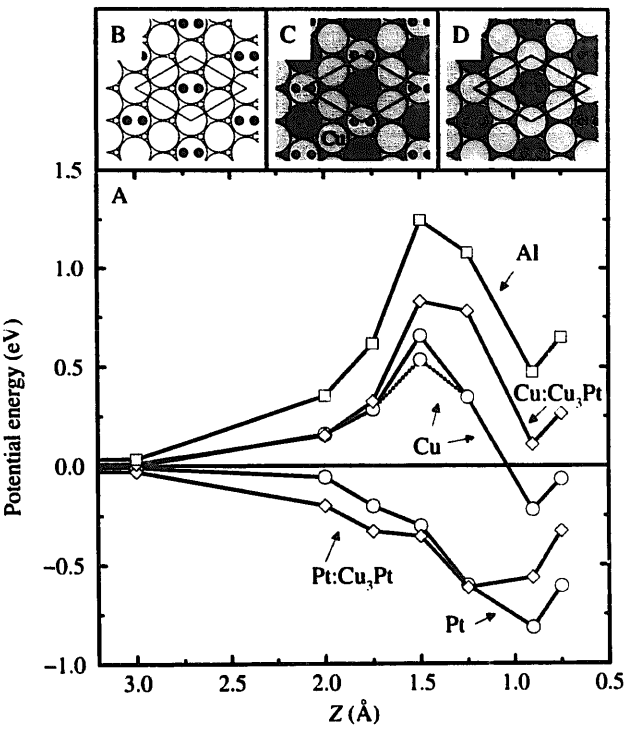

Fig. 1. (A) The potential energy along the *unrelaxed* atop reaction path. The chosen sets of H–H bond length, b, and H_2 height, Z, above the plane of the surface atomic position are: (b, Z)=(0.78 Å, 3.0 Å), (0.8 Å, 2.0 Å), (0.9 Å, 1.75 Å), (1.2 Å, 1.5 Å), (2.0 Å, 1.25 Å), ($\sqrt{2/3}a$, 0.9 Å), ($\sqrt{2/3}a$, 0.75 Å), where a is the theoretical lattice parameter of Al, Cu, Pt and Cu_3Pt respectively. The energy zero is the sum of the total energies of the separate super cell calculations of the clean slab and the isolated H_2 (b=0.78 Å) systems respectively. For Cu, the dotted line shows the energy along the path where the molecule has been allowed to move parallel to the surface and to rotate to find the minimum energy path which turns out to be for the molecule dissociating perpendicular to the Cu–Cu bridge into nearest neighbor three-fold sites [16]. (B) The geometry over Al(111), Cu(111) and Pt(111). Large open circles represent the substrate atoms, small solid circles (●) the H atoms in the H_2 molecule with b=1.2 Å. The (2×2) cell is indicated. (C) and (D) The geometry for H_2 over the Cu (light gray) and Pt (dark gray) sites in Cu_3Pt(111).

4. Electronic factors

As a starting point for our discussion of the surface properties determining the reactivity of a metal surface, consider in Fig. 2 the local density of states (DOS) projected on the d-orbitals of the Cu(111) and the Pt(111) surface atoms and the Pt and Cu atoms in the Cu_3Pt(111) surface. It can be seen that the d-bands of Cu_3Pt represent some intermediate between those of pure Cu and pure Pt; the main qualitative difference being that for the alloy, the Fermi level intersects right at the top of the d-bands. The d-bands of Cu_3Pt are therefore practically filled (i.e. there are essentially no

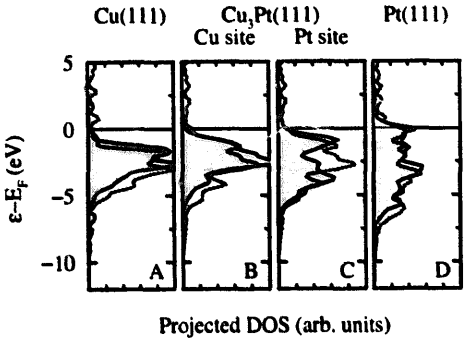

Fig. 2. The density of states (DOS) for (A) Cu, (B–C) Cu_3Pt and (D) Pt. In (A) and (B) the solid curves are the DOS projected onto the five *d*-orbitals of atomic Cu positioned in the surface, while onto the *d*-orbitals of atomic Pt in (C) and (D). The total DOS (on a different scale) for bulk Cu, Pt, and Cu_3Pt are shown by the dotted curves in the respective figures. No truncation of the atomic orbitals is used hence also some *s* character on neighboring atomic sites is measured by the solid curves and causes the background outside the energy range of the *d* bands.

d-holes!) and the DOS at the Fermi level is low compared to what it is for Pt. These properties render Pt in $Cu_3Pt(111)$ the ideal test case for reactivity theories. It is immediately clear that simple indicators of reactivity like large Fermi level DOS or localized *d*-holes just above the Fermi level cannot explain the chemistry of the Pt sites in $Cu_3Pt(111)$.

To relate the barrier for dissociation to the electronic structure of the unperturbed surface it is very tempting to build the theory on the changes in the Kohn–Sham one electron levels of density functional theory. The problem is that the total energy entering into the determination of the barrier is not related in a simple way to the sum of the one electron energies. A possible solution has been devised based on the effective medium theory. If we are not interested in the absolute magnitude of the barrier but only the *variation* from one system to the next, we can use the variational properties of the total energy functional to arrive at a very simple expression for total energy differences. If we compare the energy of an adsorbate in two different surroundings we can "freeze" the electron density and one-electron potential close to the adsorbate and use the same density and potential in the two different systems. Likewise, we can "freeze" the density and potential of the rest of space and let it be independent of the presence of the adsorbate. In that case it can be shown that the difference in interaction energy of the adsorbate in the two surroundings can be written [10,33]

$$\delta E_{ads} = \delta \int^{E_F} \varepsilon n_{ads}(\varepsilon)\, d\varepsilon + \delta E_{es}, \qquad (1)$$

where the first term is the difference in the sum of one electron energies associated with the adsorbate and the second is the difference in the electrostatic energy of the adsorbate in the two surroundings. Due to the variational principle the errors in this energy difference are second order in the errors that the "freezing" has produced in the density and potential [13,34]. If we are comparing two metals that are not too different this should be a reasonable procedure.

Eq. (1) shows that in cases where there is no large charge transfer and the electrostatic energy difference is of a minor importance, the *changes* in the barrier can be estimated from the one electron energy sum. In the following we will use this principle in two ways. First, we shall use it in conjunction with the self-consistently calculated one electron spectra to gain a qualitative understanding of the differences between the metals. Later we will also apply it in a more quantitative analysis using the frozen potential approximation directly.

We apply Eq. (1) to build a qualitative picture of the differences in activation barriers for dissociation in the following way. We consider as a common starting point an H_2 molecule at a fixed position (corresponding e.g. to the top of the barrier over the Cu(111) surface) interacting with a metal surface with only *s* and *p* electrons (Al or jellium). This interaction gives rise to a shift in the H_2 bonding (σ_g) and anti-bonding (σ_u^*) states as illustrated in Figs. 3A–3B [9,35]. The new σ_g and σ_u^* states show up as resonances in agreement with the Newns–Anderson "weak chemisorption" picture [38]. The anti-bonding state ends up just above the Fermi level while the bonding state is about 7 eV below. This is for instance illustrated by the self-consistent results for the DOS at the transition state in Fig. 4. The energy curve for the Al(111) surface in Fig. 1 shows that such a free

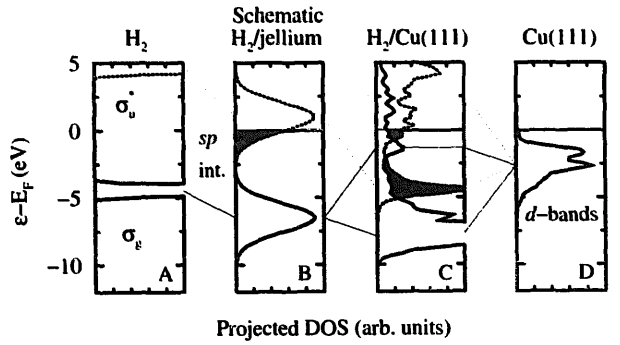

Fig. 3. Schematic drawing of the interaction between the molecular levels and the metallic states. The H_2 bonding, σ_g, and anti-bonding, σ_u^*, level (A) are broadened into resonances and shifted down due to the interaction with the metallic *s* and *p* states (B). Interaction with the metal *d*-states (D) further splits the σ_g and σ_u^* projected DOS in molecule–surface bonding and anti-bonding contributions (C). The σ_g (σ_u^*) projected DOS is shown with solid (dotted) curves and the occupied part is marked with light (dark) gray shading.

electron like surface gives rise to a considerable barrier for dissociation [35–37].

For the other metals we now have to include the effect of the metal *d*-states, and according to Eq. (1) we can estimate the *extra* energy contribution from this hybridization just from the one-electron energy differences. Fig. 3B–D shows the effect of introducing the *d*-states outside Cu(111). For both σ_g and σ_u^*, the molecule–metal *d* interaction results in the formation of two DOS features – one below and one above the center of the (renormalized) molecular levels and the center of the *d*-bands. As was demonstrated in Ref. [11] by projections onto multi-center orbitals, these DOS features represent orbitals of molecule–surface bonding and anti-bonding character. The interaction between the molecular resonance and the metal *d*-bands reflects the simplest two level interaction problem of basic chemistry, as indicated schematically by the lines between the panels in Fig. 3. This is a consequence of the narrow band width of the metal *d*-bands and can be viewed as the strong coupling limit of the Newns–Anderson model [38]. Fig. 1 shows that the effect of including the coupling to the *d*-states is to lower the barrier in all cases.

The interaction between the adsorbate states and the metal *d*-bands gives rise to a down-shift of the lowest of the two states and an up-shift of the highest state which for the parameters of interest here is given by the perturbation expression:

$$\Delta\varepsilon \sim \frac{V^2}{|\varepsilon_d - \varepsilon_\sigma|}, \qquad V \ll |\varepsilon_d - \varepsilon_\sigma|. \tag{2}$$

The effect of this interaction is then determined by three factors:

(i) The position of the molecular bonding and anti-bonding states relative to the *d*-bands ($|\varepsilon_d - \varepsilon_{\sigma_g}|$ and $|\varepsilon_d - \varepsilon_{\sigma_u^*}|$),

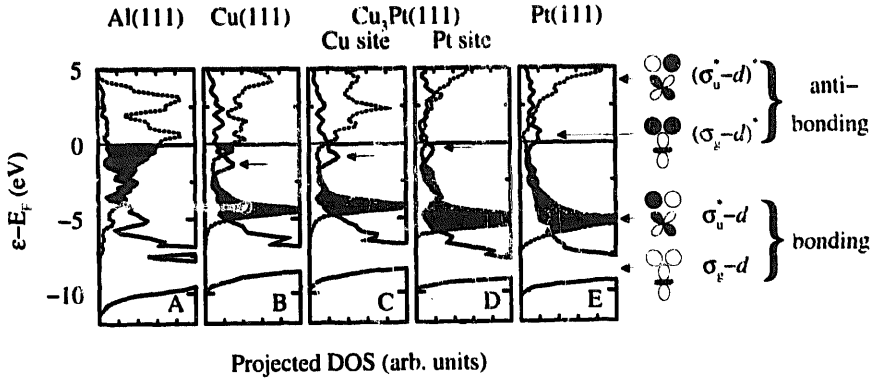

Fig. 4. The density of states (DOS) for H_2 over the atop sites of (A) Al(111), (B) Cu(111), (C) Cu in $Cu_3Pt(111)$, (D) Pt in $Cu_3Pt(111)$, and (E) Pt(111). A fixed configuration of the H_2, with an H–H separation of 1.2 Å and an H_2 height of 1.5 Å above the plane of the surface atoms, is used. The DOS is projected onto the H_2 bonding, σ_g, (solid curves) and anti-bonding, σ_u^*, (dotted curves) linear combinations of the atomic H 1*s* orbitals (truncated at 2 bohr). The arrows inside panels (B) through (E) indicate the σ_g–*d* anti-bonding states. The nature of the wavefunction at the different peaks in the DOS is depicted by the schematics at the right of the figure (the σ's – represented by two spheres – are shown atop the *d*'s with the sign of the wavefunction indicated by the shading).

(ii) The coupling matrix element V between the molecular orbitals and the metal d-states.

(iii) The filling, f, of the molecule–surface anti-bonding states given by the position of the Fermi level, E_F.

These three factors can systematically explain the behavior of the total energies given in Fig. 1. For the Cu example in Fig. 3, the σ_u^*–d interaction must be attractive, since the anti-bonding state is almost empty. The σ_g–d interaction on the other hand must be repulsive because here the anti-bonding state is filled causing a Pauli type repulsive energy term arising from the orthogonalization of the overlapping molecular and metal states. The total energy calculations shown in Fig. 1 show that the net result of the molecule–metal d interaction is lowering the energy barrier over Cu(111) relative to over Al(111).

Moving now from Cu(111) to the other metal surfaces we have to consider the changes in the interaction between the σ_g and σ_u^* and the d-states separately. The σ_u^* interaction is always attractive, since the anti-bonding σ_u^*–d state will always be above the Fermi level. The size of this interaction must be about the same outside Cu(111) and the Cu sites in $Cu_3Pt(111)$ since both the coupling strength and the position of the d-bands is about the same. Outside the Pt site in the alloy and the Pt(111) surface, the center of the d-bands is not very different from the case of Cu (cf. Fig. 2), but the coupling matrix element must be considerably larger because the 5d states are much more extended than are the 3d states. This leads to a larger attraction. Fig. 4 supports this view. The figure shows the DOS for the molecule held at 1.5 Å above the respective surfaces and sites with an H–H separation of 1.2 Å corresponding approximately to the transition state geometry over pure Cu(111). Clearly the shifts in the bonding and anti-bonding states are considerably larger outside Pt atoms than outside Cu atoms.

The σ_g interaction also changes considerably as the surface changes. The anti-bonding σ_g–d peak (indicated by the arrows in Fig. 4) just above the metal d-bands which is filled for Cu is shifted gradually above the Fermi level as the d-bands are shifted up for the Cu_3Pt and the Pt surfaces. The σ_g–d interaction thus changes sign from Cu to Pt. All in all the Pt sites show a considerably smaller (negative) barrier than the Cu sites.

Clearly, in this picture there is only a small difference between e.g. the Pt sites in $Cu_3Pt(111)$ and in Pt(111) even though there is a large difference in the local state densities just around the Fermi level for the two sites. The reason is that the molecule perturbs the surface so strongly (V is of the order eV) that it is the availability of states in a window of several eV around the Fermi level that is important for the interactions.

5. Approximate reactivity measure

We can make the arguments more quantitative by introducing as an approximate reactivity measure, δE_{ts}, the energy difference due to the coupling to the d-bands estimated directly in the frozen potential approximation. For the molecule at the transition state we write:

$$\delta E_{ts} = -2\frac{V^2}{\varepsilon_{\sigma_u^*} - \varepsilon_d} - 2(1-f)\frac{V^2}{\varepsilon_d - \varepsilon_{\sigma_g}} + \alpha V^2. \qquad (3)$$

Here the first term describes the energy gain due to the hybridization between the σ_u^* and the d-states (the factor of 2 is for spin). The second term is the corresponding σ_g–d interaction. Here there is an extra factor of $(1-f)$ because the degree of filling f of the anti-bonding state varies from one metal to the next. The last term is the repulsion due to the orthogonalization of both σ_u^* and σ_g states to the metal d-states. In both cases the orthogonalization energy will be proportional to VS where S is the overlap matrix element. In Eq. (3) we have assumed that S is proportional to V and lumped the proportionality constant into the factor α. The present reactivity measure, δE_{ts} is clearly approximate and can certainly be refined. However, the basic idea of Eq. (3), to explicitly include the direct covalent interaction between the renormalized molecular states and the metal d states is what makes this reactivity measure powerful compared to reactivity theories that only rely on the properties of the unperturbed metal surfaces [1–7]. Hoffmann has also pointed out the importance of the interaction between the molecular

states and the metal d states [8]. One important difference between his approach and the present is that rather than using the free molecular states we use the ones that have been *renormalized* to stronger binding energies through the interaction with the metal sp states [9,10]. This enables us to obtain a semi-quantitative, yet simple, estimate of the role of the d-states for the reaction energetics.

In Eq. (3) we assume that the renormalized σ_u^* level has its center above the Fermi level. As the dissociation completes, ε_{σ_g} and $\varepsilon_{\sigma_u^*}$ both converge to the position of the H adsorbate resonance, ε_H, well below the Fermi level. The frozen potential estimate of the chemisorption energy difference, δE_{chem}, for one H due to the coupling to the d-bands therefore takes the form:

$$\delta E_{chem} \sim -2(1-f)\frac{V^2}{\varepsilon_d - \varepsilon_H} + \alpha_{chem} V^2. \quad (4)$$

The $(1-f)$ dependence of the first term in this expression is able to account for the main trend in the chemisorption energies of adsorbates like H all through the transition metal series [39]. The second term in Eq. (4) is the only one active for the noble metals. Gold is the noble metal with the largest V^2 and will therefore according to Eq. (4) have the largest adsorbate s-metal d repulsion. This explains why gold – in terms of its surface reactivity – is the noblest metal [12].

In order to use Eq. (3) in the discussion of the relative reactivity of the metals, we need to evaluate ε_d, $\varepsilon_{\sigma_u^*}$, ε_{σ_g}, f, α and V^2 for the different systems. The center of the d-bands, ε_d, we readily take from Fig. 2, while the filling, f, of the anti-bonding σ_g–d state we approximate by the local filling of the surface d-states [40]. The positions, ε_{σ_g} and $\varepsilon_{\sigma_u^*}$, of the bonding and anti-bonding H_2 resonances after hybridization with the metal sp electrons, we expect to vary only little from metal to metal because the s–s coupling matrix element varies little for the metals considered [34]. We further neglect any influence of the workfunction change from one metal to the next on the renormalized H_2 levels, and measure the positions relative to the Fermi level. For the transition state configuration considered this is a reasonable approximation due to the close proximity of the H_2 and the surfaces. All in all, we take $\varepsilon_{\sigma_g} = -7$ eV and $\varepsilon_{\sigma_u^*} = 1$ eV relative to the Fermi level for all the metals. The α appearing in the orthogonalization term, we use as a single fitting parameter independent of the metal considered. Finally, but most importantly, we calculate the matrix element V within the LMTO-ASA approximation as [41]:

$$V = \eta \frac{M_H M_d}{r^3} \quad (5)$$

where M_H and M_d are given by the potential around the hydrogen and metal atoms respectively, r is the H–metal separation and η is a constant independent of the metal [42]. In the frozen potential approximation M_d is independent of the presence of the hydrogen and M_H does not depend on the metal. M_H is given by the independent estimate in Ref. [41] and the M_d's (or the potential parameters) are tabulated for all the metals in Ref. [34]. With all the terms in Eq. (3) thus accounted for, we can now get the scaling of δE_{ts} from one metal to the next. In Table 1 we show the three terms in Eq. (3) and in Fig. 5 we plot the calculated barriers for adsorption from Fig. 1 as a function of the new reactivity measure δE_{ts}. Clearly there is an excellent correlation between the two. In the table and the figure we have included results for Ni(111), NiAl(110), and Au(111) for completeness [11,12,43].

Having shown the strong correlation between the calculated energy barriers and the here proposed reactivity measure, δE_{ts}, we are now in position to discuss – on a quantitative level – which electronic factors are the most important in determining the reactivity of metal surface. Table 1 reveals that among the two attractive terms, $-2(V^2/\varepsilon_{\sigma_u^*} - \varepsilon_d)$ and $-2(1-f)(V^2/\varepsilon_d - \varepsilon_{\sigma_g})$, the former is by far the most prominent; i.e. we identify the σ_u^*–d interaction as the dominant attractive term, which can be traced to the fact that σ_u^* is initially empty. Another important observation can be made in Table 1. This is that due to the similar scaling with V of the attractive $-2(V^2/\varepsilon_{\sigma_u^*} - \varepsilon_d)$ term and the repulsive αV^2 term which represents the orthogonalization of both occupied and unoccupied adsorbate states with the metal d states, the two terms largely cancel each other. On Au, where

Table 1
The center of the *d*-bands, ε_d, measured relative to the Fermi level; the coupling strength, V^2, and the three contributions to the activation energy difference δE_{ts} in Eq. (3); all energies are in eV; the position of the anti-bonding H_2 resonance after hybridization with the metal *sp* electrons, $\varepsilon_{\sigma_u^*}$, is assumed 1 eV above the Fermi level for all the metals; likewise the position of the bonding resonance, ε_{σ_g}, is assumed 7 eV below the Fermi level; the filling, *f*, of the anti-bonding σ_g–*d* state is taken to be 1 over Cu and Au sites and to be 0.9 over Pt and Ni sites (corresponding to the degree of filling of the *d*-states in all cases) [40]; the constant α is used as a fitting parameter and takes upon the value of 0.38

Metal	ε_d	V^2	$-2\frac{V^2}{\varepsilon_{\sigma_u^*}-\varepsilon_d}$	$-2(1-f)\frac{V^2}{\varepsilon_d-\varepsilon_{\sigma_g}}$	αV^2	δE_{ts}
Cu	−2.67	2.42	−1.32	0	1.02	−0.30
Cu:Cu_3Pt	−2.35	2.42	−1.44	0	1.02	−0.42
Pt:Cu_3Pt	−2.55	9.44	−5.32	−0.42	3.96	−1.78
Pt	−2.75	9.44	−5.03	−0.44	3.96	−1.51
Ni	−1.48	2.81	−2.27	−0.10	1.18	−1.19
Ni.NiAl	−1.91	2.81	−1.93	−0.11	1.18	−0.86
Au	−3.91	8.10	−3.30	0	3.40	0.10

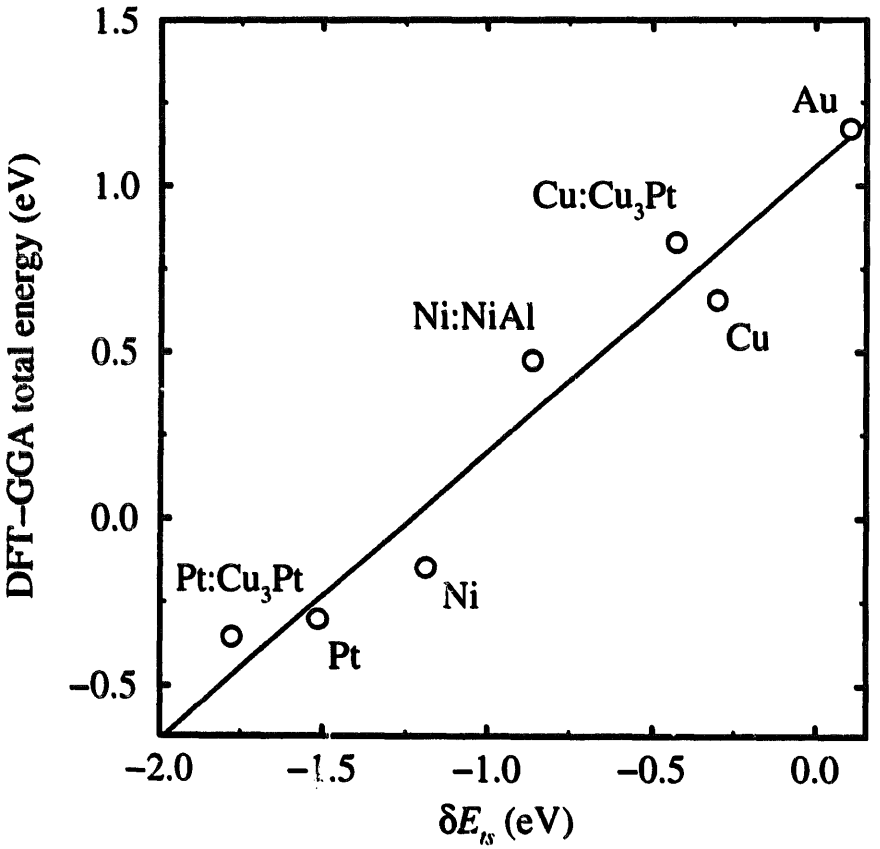

Fig. 5. Correlation between the reactivity measure δE_{ts} and the calculated activation barrier for adsorption (the total energy at (*b*, *Z*)=(1.2 Å, 1.5 Å) in Fig. 1 [43]). α in Eq. (3) has been used as a fitting parameter.

the $|\varepsilon_d-\varepsilon_{\sigma_u^*}|$ is larger than on any other metal surface considered, the attractive term, through large in absolute numbers, is therefore small relative to the repulsive term and the two therefore almost completely cancel each other leaving the Au surface with a large barrier despite the presence

of *d*-states actively involved in the chemical reaction.

6. Conclusions

We conclude that to understand the trends in reactivity of H_2 outside transition and noble metals and their alloys, one has to consider the interaction between the metal *d*-states and the bonding and anti-bonding molecular states after they have been shifted due to the interaction with the free-electron-like metallic electrons. It then turns out that the important surface parameters determining the reactivity are the position of the whole *d*-bands relative to the Fermi level, because this determines both the size of the bonding and anti-bonding energy shifts and the degree of filling of the anti-bonding states as well as the size of the coupling matrix elements which also enter into the size of the energy shifts. We expect that this picture can be transferred directly to other adsorbing molecules and surfaces, but more calculations are required to test this out in detail.

Acknowledgements

These calculations have only been possible due to the computational resources of the JRCAT supercomputing system, which is supported by the New Energy and Industrial Technology Development Organization (NEDO) of Japan. Center for Atomic-scale Materials Physics (CAMP) is sponsored by the Danish National Research Foundation. This work was supported in part by the Danish Research Councils through the Center for Surface Reactivity.

References

[1] P.J. Feibelman and D. Hamann, Phys. Rev. Lett. 52 (1984) 61; Surf. Sci. 149 (1985) 48.
[2] L.M. Falicov and G.A. Somorjai, Proc. Nat. Acad. Sci. USA 82 (1985) 2207.
[3] W. Yang and R.G. Parr, Proc. Nat. Acad. Sci. USA 82 (1985) 6723.
[4] J. Harris and S. Andersson, Phys. Rev. Lett. 55 (1985) 1583.
[5] K. Fukui, T. Yonezawa and H. Shingu, J. Chem. Phys. 20 (1952) 722.
[6] R.G. Parr and W. Yang, Density Functional Theory of Atoms and Molecules (Oxford Univ. Press, New York, 1989).
[7] M.H. Cohen, M.V. Ganduglia-Pirovano and J. Kudrnovsky, Phys. Rev. Lett. 72 (1994) 3222; M.H. Cohen, M.V. Ganduglia-Pirovano and J. Kudrnovsky, J. Chem. Phys. 101 (1994) 8988.
[8] R. Hoffmann, Rev. Mod. Phys. 60 (1988) 601.
[9] B.I. Lundqvist, O. Gunnarsson, H. Hjelmberg and J.K. Nørskov, Surf. Sci. 89 (1979) 196.
[10] S. Holloway, B.I. Lundqvist and J.K. Nørskov, Proc. Int. Congress on Catalysis, Berlin, Vol. 4 (1984), p. 85; J.K. Nørskov, Rep. Prog. Phys. 53 (1990) 1253.
[11] B. Hammer and M. Scheffler, Phys. Rev. Lett. 74 (1995) 3487.
[12] B. Hammer and J.K. Nørskov, Nature 376 (1995) 238.
[13] K.W. Jacobsen, J.K. Nørskov and M.J. Puska, Phys. Rev. B 35 (1987) 7423.
[14] D.M. Ceperley and B.J. Alder, Phys. Rev. Lett 45 (1980) 566; J.P. Perdew and A. Zunger, Phys. Rev. B 23 (1981) 5048.
[15] J.P. Perdew, J.A. Chevary, S.H. Vosko, K.A. Jackson, M.R. Pederson, D.J. Singh and C. Fiolhais, Phys. Rev. B 46 (1992) 6671.
[16] B. Hammer, M. Scheffler, K.W. Jacobsen and J.K. Nørskov, Phys. Rev. Lett. 73 (1994) 1400.
[17] J.A. White, D.M. Bird, M.C. Payne and I. Stich, Phys. Rev. Lett. 73 (1994) 1404.
[18] P.H.T. Philipsen, G. te Velde and E.J. Baerends, Chem. Phys. Lett. 226 (1994) 583.
[19] P. Hu, D.A. King, S. Crampin, M.-H. Lee and M.C. Payne, Chem. Phys. Lett. 230 (1994) 501.
[20] A. Gross, B. Hammer, M. Scheffler and W. Brenig, Phys. Rev. Lett. 73 (1994) 3121.
[21] R. Linke, U. Schneider, H. Busse, C. Becker, U. Schröder, G.R. Castro and K. Wandelt, Surf. Sci. 307–309 (1994) 407.
[22] F. Jona and P.M. Marcus, in: The Structure of Surfaces II, Eds. J.F. van der Veen and M.A. Van Hove (Springer, Berlin, 1988) p. 90.
[23] J. Neugebauer and M. Scheffler, Phys. Rev. B 46 (1992) 16067.
[24] M.C. Payne, M.P. Teter, D.C. Allan, T.A. Arias and J.D. Joannopoulos, Rev. Mod. Phys. 64 (1992) 1045.
[25] M.J. Gillan, J. Phys.: Condens. Matter 1 (1989) 689.
[26] D.J. Chadi and M.L. Cohen, Phys. Rev. B 8 (1973) 5747; S.L. Cunningham, Phys. Rev. B 10 (1974) 4988.
[27] G.B. Bachelet, D.R. Hamann and M. Schlüter, Phys. Rev. B 26 (1982) 4199.
[28] N. Troullier and J.L. Martins, Phys. Rev. B 43 (1991) 1993; For the Pt *s* and *d* potentials $r_c = 2.26$ bohr and a $6s^1 5d^9$ atomic configuration are used, while for the *p* potential $r_c = 2.50$ bohr and $6s^{0.75} 6p^{0.25} 5d^8$ are used.

[29] Unlike the barrier height, we expect the heats of dissociative H_2 chemisorption (i.e. the minima in Fig. 1A) to be quite sensitive to relaxations in the H coordinates parallel to the surface – in particular for Al(111) and Cu_3Pt. For H on Al(110), for instance the lowest energy site is on top and the chemisorption energy is +0.1 eV [36] rather than +0.5 eV for the threefold site in Fig. 1A.

[30] H.A. Michelsen, C.T. Rettner and D.J. Auerbach, Phys. Rev. Lett. 69 (1992) 2678;
H.A. Michelsen, C.T. Rettner, D.J. Auerbach and R.N. Zare, J. Chem. Phys. 98 (1993) 8294.

[31] H.F. Berger and K.D. Rendulic, Surf. Sci. 253 (1991) 325.

[32] K. Christmann, Surf. Sci. Rep. 9 (1988) 1;
J.K. Brown, A. Luntz and P.A. Schultz, J. Chem. Phys. 95 (1991) 3767.

[33] For a detailed derivation see e.g.: J.K. Nørskov, in: Physics and Chemistry of Alkali Metal Adsorption, Eds. H.P. Bonzel, A.M. Bradshaw and G. Ertl (Elsevier, Amsterdam, 1989) p. 253.

[34] O.K. Andersen, O. Jepsen and D. Glötzel, Highlights of Condensed Matter Theory LXXXIX Corso Soc. Italiana di Fisica, Bologna (1985) p. 59.

[35] J.K. Nørskov, A. Houmøller, P.K. Johansson and B.I. Lundqvist, Phys. Rev. Lett. 46 (1981) 257.

[36] B. Hammer, K.W. Jacobsen and J.K. Nørskov, Phys. Rev. Lett. 70 (1993) 3971;
K. Gundersen, K.W. Jacobsen, J.K. Nørskov and B. Hammer, Surf. Sci. 304 (1994) 131.

[37] D.M. Bird, L.J. Clarke, M.C. Payne and I. Stich, Chem. Phys. Lett. 212 (1993) 518.

[38] D.M. Newns, Phys. Rev. 178 (1969) 1123.

[39] P. Nordlander, S. Holloway and J.K. Nørskov, Surf. Sci. 136 (1984) 59.

[40] Note here the difference between the filling of the d-bands and the local filling of the d-states. While the d-bands of Cu_3Pt are filled, we find a filling of the d-projected density of states of 0.94, close to the value for the Pt surface of 0.92. For simplicity we therefore use a value of 0.9 (the "ideal" filling) for all Pt (and Ni) sites.

[41] J.K. Nørskov, J. Chem. Phys. 90 (1989) 7461.

[42] η contains the geometry and the angular momentum dependent Slater–Koster terms between the two H 1S orbitals and the relevant d-orbitals. Composing the σ_g and σ_u^* as LCAOs of the H 1S we obtain:

$$\eta_{\sigma_u^*-d_{xz}}=\sqrt{\frac{2}{1-S_{HH}}}\,\frac{\sqrt{3}(l^2-m^2)}{2}\,2\sqrt{5},\quad l=\frac{Z}{r},\quad m=\frac{b/2}{r},$$

$$\eta_{\sigma_g-d_{z^2}}=\sqrt{\frac{2}{1+S_{HH}}}\,\frac{1-3n^2}{2}\,2\sqrt{5},\quad n=\frac{b/2}{r},$$

where S_{HH} is the overlap between two H 1s at the separation b. Depending on the value of S_{HH}, $\eta_{\sigma_u^*-d_{xz}}$ and $\eta_{\sigma_g-d_{z^2}}$ are quite similar. As η is independent of the metal, it serves to consider one common η and thereby only one V for the purpose of investigating the scaling of δE_{ts} as a function of the metal. Using the average of $\eta_{\sigma_u^*-d_{xz}}$ and $\eta_{\sigma_g-d_{z^2}}$ and neglecting S_{HH} the V becomes: 0.246 bohr$^{-3}M_HM_d$ at $(b, Z)=(1.2\text{ Å}, 1.5\text{ Å})$.

[43] For the H_2 on NiAl(110) we use the calculated value from Ref. [11] where the (b, Z) is (1.5 Å, 1.33 Å) including in Z the −0.14 Å relaxation of the surface Ni atom.